THE ASTROPHYSICAL JOURNAL, 587:L5–L8, 2003 April 10

A RADIO FLARE FROM GRB 020405: EVIDENCE FOR A UNIFORM MEDIUM AROUND A MASSIVE STELLAR PROGENITOR

E. BERGER,[1] A. M. SODERBERG,[1] D. A. FRAIL,[2] AND S. R. KULKARNI[1]
Received 2003 January 30; accepted 2003 March 6; published 2003 March 12

ABSTRACT

We present radio observations of GRB 020405 starting 1.2 days after the burst that reveal a rapidly fading "radio flare." Based on its temporal and spectral properties, we interpret the radio flare as emission from the reverse shock. This scenario rules out a circumburst medium with a radial density profile $\rho \propto r^{-2}$ expected around a mass-losing massive star since in that case, the reverse-shock emission decays on the timescale of the burst duration $t \sim 10^2$ s. Using published optical and X-ray data, along with the radio data presented here, we further show that a self-consistent model requires collimated ejecta with an opening angle, $\theta_j \sim 6°$ ($t_j \approx 0.95$ days). As a consequence of the early jet break, the late-time ($t > 10$ days) emission measured with the *Hubble Space Telescope* significantly deviates from an extrapolation of the early, ground-based data. This, along with an unusually red spectrum, $F_\nu \propto \nu^{-3.9}$, strengthens the case for a supernova that exploded at about the same time as GRB 020405, thus pointing to a massive stellar progenitor for this burst. This is the first clear association of a massive progenitor with a uniform medium, indicating that a $\rho \propto r^{-2}$ profile is not a required signature and, in fact, may not be present on the length scales probed by the afterglow in the majority of bursts.

Subject headings: gamma rays: bursts — stars: mass loss

1. INTRODUCTION

Over the past few years, several indirect lines of evidence have emerged in favor of massive stars as the progenitors of long-duration gamma-ray bursts (GRBs; e.g., Berger, Kulkarni, & Frail 2001; Galama & Wijers 2001; Bloom, Kulkarni, & Djorgovski 2002). Perhaps the most convincing evidence comes from the detection of late-time ($t \sim 20$ days) red bumps in several optical afterglows (e.g., Bloom et al. 1999). While several interpretations of these bumps have been suggested (Esin & Blandford 2000; Waxman & Draine 2000; Ramirez-Ruiz et al. 2001), the preponderance of spectral and temporal evidence (e.g., Bloom et al. 2002; Garnavich et al. 2003) indicates that these bumps are due to emission from supernovae (SNe) accompanying the bursts. These observations lend support to the collapsar model (Woosley 1993; MacFadyen & Woosley 1999), in which the core of a massive star collapses to a black hole, which then accretes matter and powers the GRB while the rest of the star produces an SN.

A seemingly unavoidable consequence of this scenario is that the GRB ejecta should expand into a medium modified by mass loss from the progenitor star. To first order, the expected density profile is $\rho \propto r^{-2}$, arising from a constant mass-loss rate and wind velocity. Extensive efforts have been made to find evidence of such a density profile based on broadband observations of the afterglow emission (e.g., Chevalier & Li 2000; Panaitescu & Kumar 2002). Unfortunately, these studies have been inconclusive in distinguishing between a wind density profile and a medium with uniform density, due in part to the lack of early radio and submillimeter observations. Thus, the signature of stellar mass loss remains the elusive missing link in the association of GRBs and massive stars.

To date, the single exception to this disappointing trend is GRB 011121, which provides strong evidence of a circumburst medium shaped by a stellar wind (Price et al. 2002) and an accompanying SN (Bloom et al. 2002; Garnavich et al. 2003). The reason for these unambiguous results is the combination of exquisite *Hubble Space Telescope* (*HST*) observations, extensive near-IR data, and dual-band radio data.

More recently, Price et al. (2003) presented the gamma-ray properties and redshift ($z = 0.695 \pm 0.005$) of GRB 020405, along with multiband ground-based and *HST* optical observations. The observations between 15 and 65 days after the burst reveal a red bump (with a spectrum $F_\nu \propto \nu^{-3.9}$) brighter than an extrapolation of the early data. Price et al. (2003) interpret this emission as coming from an SN accompanying the burst, but note that the statistical significance of this result depends on the degree of collimation of the GRB ejecta. This is because a more collimated outflow results in an earlier steepening of the afterglow light curves, and hence a more significant deviation at late time.

In this Letter, we present radio observations of GRB 020405 that point to a uniform circumburst medium. We also show that the radio, optical, and X-ray (Mirabal, Paerels, & Halpern 2003) data require an early jet break, which significantly strengthens the SN interpretation. Combining these two results, we conclude that a $\rho \propto r^{-2}$ density profile is not a required signature of a massive stellar progenitor.

2. RADIO OBSERVATIONS

We initiated Very Large Array (VLA[3]) observations 1.2 days after the burst using the standard continuum mode with 2×50 MHz contiguous bands. A log of all observations is given in Table 1. We used the extragalactic source 3C 286 (J1331+305) for flux calibration, while the phase was monitored using J1356−343.

3. REVERSE-SHOCK EMISSION IN THE RADIO BAND

In Figure 1, we plot the 8.46 GHz light curve of GRB 020405 as well as the radio spectrum between 1.43 and 8.46 GHz on

[1] Division of Physics, Mathematics, and Astronomy, MS 105-24, California Institute of Technology, Pasadena, CA 91125.
[2] National Radio Astronomy Observatory, P.O. Box O, 1003 Lopezville Road, Socorro, NM 87801.

[3] The VLA is operated by the National Radio Astronomy Observatory, which is a facility of the National Science Foundation operated under cooperative agreement by Associated Universities, Inc.

TABLE 1
VLA Radio Observations of GRB 020405

Epoch (UT)	Δt (days)	ν_0 (GHz)	Flux Density (μJy)
Apr 6.22	1.19	8.46	481 ± 36
Apr 6.25	1.22	22.5	<300
Apr 8.36	3.33	8.46	157 ± 43
Apr 8.38	3.35	4.86	160 ± 51
Apr 8.40	3.37	1.43	234 ± 77
Apr 8.42	3.39	22.5	<600
Apr 9.40	4.37	8.46	121 ± 39
Apr 10.28	5.25	8.46	83 ± 18
Apr 13.24	8.21	8.46	47 ± 27
Apr 21.28	16.3	8.46	115 ± 21
May 7.20	32.2	8.46	64 ± 20
May 21.12	46.1	8.46	61 ± 26
May 24.13	49.1	8.46	−9 ± 20
May 27.17	52.1	8.46	−11 ± 25
May 21.12–27.17	46.1–52.1	8.46	0 ± 14

Note.—The columns are, from left to right, the UT date of each observation, the time since the burst, the observing frequency, and the flux density at the position of the radio transient with the rms noise calculated from each image. The last row gives the flux density at 8.46 GHz from a co-added map of the data from May 21 to 27.

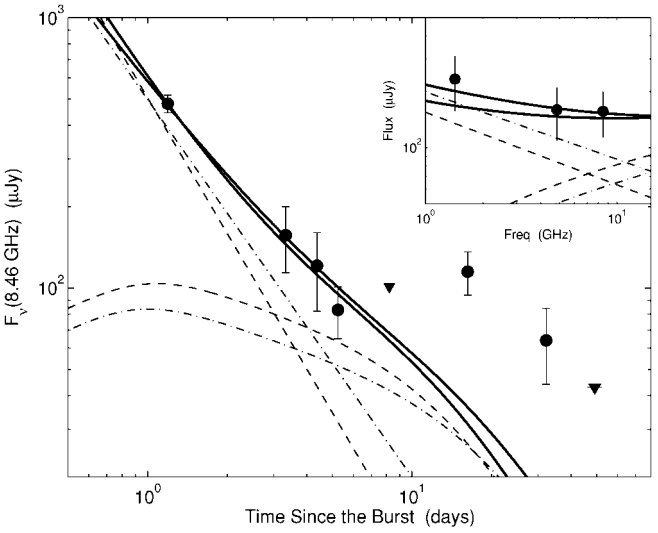

Fig. 1.—Radio light curve at 8.46 GHz and the spectrum between 1.4 and 8.5 GHz on day 3.3 (*inset*). The solid lines represent the best-fit combined emission from the reverse- and forward-shock model described in § 4 for the thin and thick shell cases. The dashed (thin shell) and dash-dotted (thick shell) lines show the contributions of the reverse and forward shocks separately.

day 3.3. The early emission is characterized by two important features. First, it is brightest ($F_\nu \approx 0.5$ mJy) during the first observation ($t \approx 1.2$ days) and rapidly fades, $F_\nu \propto t^{-1.2\pm0.4}$, between 1.2 and 5 days. Second, the spectral index between 1.43 and 8.46 at $t \approx 3.3$ days is $\beta_{\rm rad} \approx -0.3 \pm 0.3$, and similarly at $t \approx 1.2$ days $\beta_{\rm rad} < -0.5$ between 8.46 and 22.5 GHz.

The rapid fading and negative spectral slope are atypical for emission from the forward shock on the timescale of 1 day. In fact, with typical parameters, the radio band, $\nu_{\rm rad}$, lies well below the peak of the synchrotron spectrum at early time, $\nu_m \approx 260\epsilon_{B,-2}^{1/2}\epsilon_{e,-1}^{2}E_{52}^{1/2}t_d^{-3/2}$ GHz (Sari & Esin 2001); here $\epsilon_B = 0.01\epsilon_{B,-2}$ and $\epsilon_e = 0.1\epsilon_{e,-1}$ are the fractions of shock energy in the magnetic fields and electrons, respectively, and $E = 10^{52}E_{52}$ is the afterglow kinetic energy. In this regime, the spectrum is $F_\nu \propto \nu^{1/3}$ (or $F_\nu \propto \nu^2$ if $\nu_{\rm rad} < \nu_a$, the synchrotron self-absorption frequency). As a result, the early radio flux is expected to either increase, as $t^{1/2}$ or t^1 (Sari, Piran, & Narayan 1998; Chevalier & Li 2000), be flat (Chevalier & Li 2000), or decay as $t^{-1/3}$ (Sari, Piran, & Halpern 1999), followed by a steep decline as t^{-1} to t^{-2} when ν_m crosses the radio band. This behavior is observed in most radio afterglows (e.g., Berger et al. 2000), and since the early radio emission from GRB 020405 does not follow this general trend, we conclude that it did not arise from the forward shock.

Instead, we interpret the observed emission as coming from a reverse shock (Mészáros & Rees 1997; Sari & Piran 1999b) plowing back into the relativistic ejecta. Similar "radio flares" have been observed in several afterglows (e.g., Kulkarni et al. 1999), in particular from GRB 990123 where the flare was shown to be the low-energy tail of the $V \approx 9$ mag optical flash at $t \sim 50$ s (Kulkarni et al. 1999; Sari & Piran 1999a). In all cases in which a radio flare has been observed, the emission had similar properties to that from GRB 020405, namely, bright ($F_\nu \sim 0.5$ mJy) emission measured at early time ($t \sim 1$ day) followed by a rapid decline.

Hydrodynamical studies of the reverse shock (e.g., Kobayashi & Sari 2000) have shown that the radio emission depends on the properties of the ejecta and circumburst medium. In particular, the main implication of the radio flare from GRB 020405 is that it effectively rules out a circumburst medium with a density profile $\rho \propto r^{-2}$ (hereafter Wind). Chevalier & Li (2000) have shown that in a Wind environment, the cooling frequency of the reverse shock, $\nu_{c,\rm RS} \sim 4 \times 10^8 t_{\rm sec}$ Hz, is significantly lower than its characteristic frequency, $\nu_{m,\rm RS} \sim 10^{19}t_{\rm sec}^{-1}$ Hz. Thus, the flux is independent of time until the reverse shock crosses the shell at $t_{\rm cr} = 5(1+z)\Delta_{10}$ s (Chevalier & Li 2000); here $\Delta = 10\Delta_{10}$ lt-s is the initial width of the shell. Following the shell crossing, electrons are no longer accelerated, and since the reverse shock is highly radiative ($\nu_{c,\rm RS} \ll \nu_{m,\rm RS}$), the emission decays exponentially. Thus, strong emission from the reverse shock at $t \sim 1$–2 days is not expected in a Wind environment, indicating that the early radio emission from GRB 020405 requires a circumburst medium with uniform density (hereafter ISM).

In addition, the flat spectral slope between 1.4 and 8.5 GHz measured at $t = 3.3$ days indicates that for both the reverse and forward shocks, $\nu_a \lesssim 1.4$ GHz. Otherwise, the emission from the reverse shock would be severely attenuated by the forward shock, $F_{\nu,\rm obs} = F_{\nu,\rm em}e^{-\tau_\nu}$, resulting in a significantly steeper spectrum; here τ_ν is the synchrotron optical depth.

4. UNIFORM DENSITY MODELS FOR THE AFTERGLOW EMISSION

Using the conditions inferred in § 3, we model the radio, optical, and X-ray data with a model describing self-consistently the time evolution of the forward and reverse shocks in a uniform medium. We consider the optical data only at $t < 10$ days since the emission at later times is dominated by a much redder component, possibly an SN. We return to this point in § 5.

The time evolution of the reverse-shock spectrum ($F_\nu \propto \nu^{1/3}$ for $\nu < \nu_{m,\rm RS}$ and $F_\nu \propto \nu^{-(p-1)/2}$ for $\nu > \nu_{m,\rm RS}$) is described by $\nu_{m,\rm RS} \propto t^{-3(8+5g)/7(1+2g)}$, $F_{\nu,0,\rm RS} \propto t^{-(12+11g)/7(1+2g)}$, and the time of peak emission, $t_p = \max[t_{\rm dur}/(1+z), t_{\rm dec}]$ (Kobayashi & Sari 2000); here $t_{\rm dur} = 60$ s is the duration of GRB 020405 (Price et al. 2003), $t_{\rm dec} = (3E/32\pi\Gamma_0^8 n_0 m_p c^2)^{1/3}$, Γ_0 is the initial Lorentz factor, and n_0 is the circumburst density. The parameter $3/2 \le g \le 7/2$ describes the evolution of the reverse-shock Lorentz factor, $\Gamma \propto r^{-g}$, and the limits correspond to the adiabatic expansion ($g = 3/2$) and pressure equilibrium between the for-

TABLE 2
UNIFORM DENSITY JET MODELS FOR GRB 020405

Parameter	Thin Shell	Thick Shell
ν_a (Hz)	10^9	10^9
ν_m (Hz)	1.9×10^{12}	4.0×10^{12}
ν_c (Hz)	3.5×10^{14}	1.0×10^{14}
$F_{\nu,0}$ (μJy)	740	760
p	1.78	1.73
t_j (days)	0.99	0.91
$A_V^{\rm host}$ (mag)	0.28	0.25
Γ_0[a]	1.2×10^3	3.2×10^3
$\chi^2_{\rm min}$/dof	61.2/61	58.7/61
$E_{\rm iso,52}$	0.3	0.2
n_0	0.05	0.08
ϵ_e	0.1	0.1
ϵ_B	0.3	0.7

NOTE.—Best-fit synchrotron parameters and the inferred physical parameters for the reverse- and forward-shock model described in § 4. The quoted values for the forward shock are at $t = t_j$. We give the results for the thin shell (with $g = 3/2$) and thick shell (with $g = 7/2$) cases. In both models, we fix the value of ν_a at 1 GHz based on the flat spectrum in the radio band between 1.4 and 8.5 GHz (§ 3).

[a] Γ_0 is not well constrained and can take a wide range of values (Fig. 3).

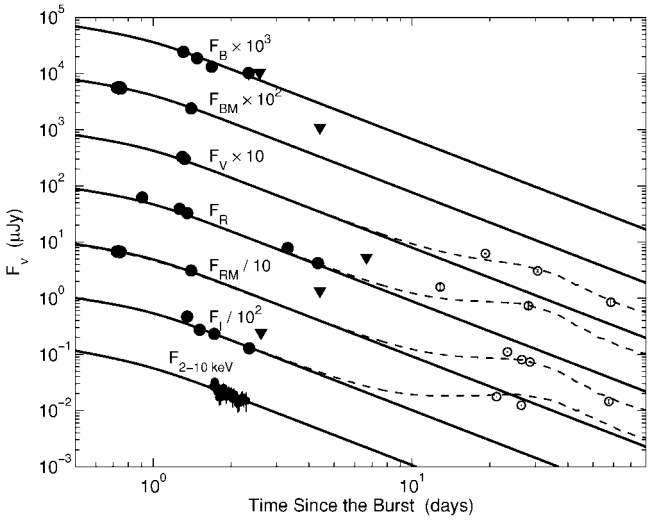

FIG. 2.—Optical and X-ray light curves of GRB 020405. The filled triangles represent upper limits, while the open circles represent late-time observations, dominated by emission from an SN. The solid lines represent the best-fit reverse- and forward shock-model described in § 4, and the dashed lines represent the combined afterglow flux and flux from SN 1998bw redshifted to $z = 0.695$.

ward and reverse shocks ($g = 7/2$). To evaluate t_p, $\nu_{m,\rm RS}(t_p)$, and $F_{\nu,0,\rm RS}(t_p)$, we use the physical parameters inferred from the forward-shock emission (see below and Table 2), in conjunction with equations (7)–(9) of Kobayashi (2000) for the thick shell case (i.e., when the reverse shock is relativistic and effectively decelerates the shell) and their equations (15)–(17) for the thin shell case (i.e., when the reverse shock cannot decelerate the shell effectively). We set the nominal values of $g = 3/2$ and 7/2 for the thin and thick shell cases, respectively, so that the only free parameter is Γ_0.

For the forward shock, we use the time evolution of the synchrotron spectrum in the appropriate regime (i.e., the spherical ISM for $t < t_j$ and an expanding jet for $t > t_j$); here t_j, the jet break time, is the epoch at which $\Gamma \sim \theta_j^{-1}$, and θ_j is the half-opening angle of the jet. To account for extinction within the host galaxy, we use the parametric extinction curves presented by Reichart (2001).

The results for the thin and thick shell models are shown in Figures 1 and 2 and are summarized in Table 2. We find that both models provide an equally adequate fit (with $\chi^2_{\rm min} \approx 1$ per degree of freedom [dof]), with an estimated uncertainty of about 5%–10% in the derived parameters. The single exception is Γ_0, which is not well constrained, $\Gamma_0 \sim 60$–5×10^3 (Fig. 3). The value of $p \approx 1.7$–1.8 is somewhat lower than the typical $p \sim 2$ observed in other well-studied bursts (e.g., Panaitescu & Kumar 2002), but this is no cause for concern since (1) our value is consistent with $p = 2$ within the uncertainty and (2) the spectral index of the X-ray emission, $\beta_{\rm X} = -0.72 \pm 0.21$ (Mirabal et al. 2003), indicates $p = 1.44 \pm 0.42$ (given that $\nu_{\rm X} > \nu_c$).

More importantly, both models require collimated ejecta with $t_j \approx 0.95$ day (hereafter Jet). Models with a significantly wider collimation angle have $\chi^2_{\rm min} \sim 10$/dof, primarily because they severely underestimate the flux in the X-ray band and cannot explain the radio and optical emission simultaneously. In particular, Masetti, Palazzi, & Pian (2003), using only optical/near-IR data and ignoring the radio emission, claim that $t_j > 10$ days. They measure a flux of 55 μJy in the I band at $t = 18.8$ hr with $\alpha = -1.54$. Since with typical parameters (Sari et al. 1998) ν_m crosses the optical bands at $t \sim 1$ hr, their model indicates that the radio emission should peak with a flux of about 5 mJy at $t \approx 50$ days, in direct contradiction to the data.

At the same time, our model underestimates the radio flux at $t \gtrsim 15$ days by about 4 σ on day 16.3 and by about 2.5 σ on day 32. This is due to an apparent brightening of the radio emission on this timescale. Since in the radio band $F_\nu \propto n_0^{1/2}$, one possible explanation is that the forward shock encounters a density enhancement; an increase by a factor of 10 is required. The flux in the optical bands would remain largely unaffected since $\nu_{\rm opt} < \nu_c$ (see Table 2), in which case the flux is independent of density.

5. THE PROGENITOR OF GRB 020405 AND GRB CIRCUMBURST ENVIRONMENTS

In the previous section, we did not consider the optical emission at $t \gtrsim 10$ days since it has a distinct spectrum $F_\nu \propto$

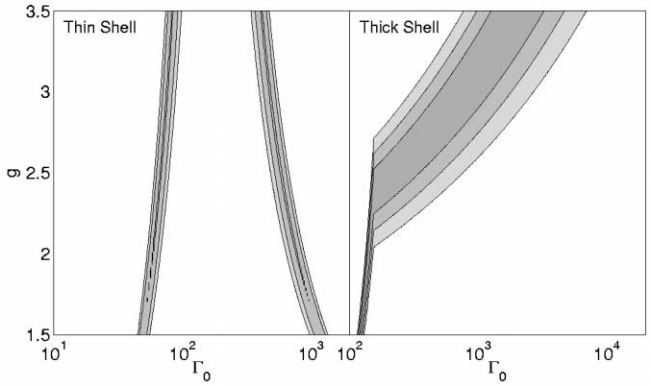

FIG. 3.—Contours (1, 2, and 3 σ) of Γ_0 vs. g based on the best-fit models for the reverse- and forward-shock emission in the thin and thick shell cases (Table 2). Both Γ_0 and g are not well constrained. In particular, Γ_0 has two sets of minima in the thin shell case, corresponding to the cases when $t_p = t_{\rm dec}$ and $t_p = t_{\rm dur}/(1+z)$.

$\beta^{-3.9\pm0.1}$ compared with $F_\nu \propto \beta^{-1.15\pm0.07}$ for the early afterglow. Moreover, the flux measured with *HST* exceeds the predicted brightness of the afterglow by a factor of about 3–5 in the *R* and *I* bands (Fig. 2). These two observations indicate that the late-time emission comes from a separate component.

Price et al. (2003) interpret this emission as coming from an SN but noted that the significance of this result depends sensitively on the time of the jet break. Our model with $t_j \approx 0.95$ day indicates that the SN interpretation is secure.

This is also supported by a comparison with SN 1998bw (Galama et al. 1998). In Figure 2, we plot the combined emission from the afterglow of GRB 020405 and SN 1998bw redshifted to $z = 0.695$. The SN light curves are corrected for Galactic extinction, $E(B-V) = 0.054$ mag (Schlegel, Finkbeiner, & Davis 1998), as well as extinction within the host galaxy as determined in § 4. While SN 1998bw does not provide a perfect fit to the data, the level of agreement is remarkable given that there are other effects at play (e.g., an earlier decay for a fainter luminosity; Iwamoto et al. 1998).

The conclusion that GRB 020405 was accompanied by an SN indicates that the progenitor must have been a massive star. However, we also demonstrated that the circumburst density profile is uniform, at least in the range $r \sim 10^{15}$–10^{17} cm. This is the first case in which a massive progenitor and a uniform ambient medium have been associated directly, leading us to conclude that a strong density gradient, $\rho \propto r^{-2}$, on the length scales probed by the afterglow is not a required signature of such progenitors. In fact, this may explain why the signature of stellar mass loss has not been observed in the majority of afterglows.

The uniform medium around the progenitor of GRB 020405 does not imply that the progenitor did not lose mass. In fact, it has been suggested that a relatively uniform medium can occur downstream from the wind termination shock (Ramirez-Ruiz et al. 2001). This region can extend out to 10^{18} cm. In addition, a density enhancement is expected at the termination shock, which can explain the increased radio flux at $t \gtrsim 15$ days compared with our model predictions (§ 4).

6. CONCLUSIONS

We show that the early radio emission from GRB 020405 was dominated by the reverse shock and that this directly implies a uniform circumburst medium. The same conclusion holds for all bursts in which radio flares have been detected on the timescale of ~1 day. The broadband data indicate that the ejecta underwent a jet break at $t \approx 0.95$ days (i.e., $\theta_j \sim 6°$), resulting in a significant deviation of the late-time optical emission measured with *HST* from an extrapolation of the model. Combined with the spectral properties of the late emission, and a reasonable agreement with the optical emission of SN 1998bw, this indicates that GRB 020405 was accompanied by an SN. Thus, the progenitor of this burst was a massive star.

The association of a massive stellar progenitor with a uniform circumburst medium indicates that the tedious search for a $\rho \propto r^{-2}$ density profile may have been partly in vain. It appears that a Wind profile does not necessarily accompany every GRB and in fact may not be the case for the majority of bursts. This result, in conjunction with the inferred Wind medium for GRB 011121, which was also accompanied by an SN, indicates that the circumburst environments of GRBs are more diverse than the simple assumption of a constant mass-loss rate and wind velocity; the interaction of the wind with the local environment may play a significant role. Deeper insight into the structure of the circumburst medium requires rapid localizations, dense multiband follow-up, and self-consistent modeling of the emission in all bands.

E. B. thanks R. Chevalier and R. Sari for valuable discussions. We acknowledge support from NSF and NASA grants.

REFERENCES

Berger, E., Kulkarni, S. R., & Frail, D. A. 2001, ApJ, 560, 652
Berger, E., et al. 2000, ApJ, 545, 56
Bloom, J. S., Kulkarni, S. R., & Djorgovski, S. G. 2002, AJ, 123, 1111
Bloom, J. S., et al. 1999, Nature, 401, 453
———. 2002, ApJ, 572, L45
Chevalier, R. A., & Li, Z. 2000, ApJ, 536, 195
Esin, A. A., & Blandford, R. 2000, ApJ, 534, L151
Galama, T. J., et al. 1998, Nature, 395, 670
Galama, T. J., & Wijers, R. A. M. J. 2001, ApJ, 549, L209
Garnavich, P. M., et al. 2003, ApJ, 582, 924
Iwamoto, K., et al. 1998, Nature, 395, 672
Kobayashi, S. 2000, ApJ, 545, 807
Kobayashi, S., & Sari, R. 2000, ApJ, 542, 819
Kulkarni, S. R., et al. 1999, ApJ, 522, L97
MacFadyen, A. I., & Woosley, S. E. 1999, ApJ, 524, 262
Masetti, N., Palazzi, E., & Pian, E. 2003, A&A, submitted (astro-ph/0302350)
Mészáros, P., & Rees, M. J. 1997, ApJ, 476, 232
Mirabal, N., Paerels, F., & Halpern, J. P. 2003, ApJ, in press (astro-ph/0209516)
Panaitescu, A., & Kumar, P. 2002, ApJ, 571, 779
Price, P. A., et al. 2002, ApJ, 572, L51
———. 2003, ApJ, in press (astro-ph/0208008)
Ramirez-Ruiz, E., Dray, L. M., Madau, P., & Tout, C. A. 2001, MNRAS, 327, 829
Reichart, D. E. 2001, ApJ, 554, 643
Sari, R., & Esin, A. A. 2001, ApJ, 548, 787
Sari, R., & Piran, T. 1999a, ApJ, 517, L109
———. 1999b, ApJ, 520, 641
Sari, R., Piran, T., & Halpern, J. P. 1999, ApJ, 519, L17
Sari, R., Piran, T., & Narayan, R. 1998, ApJ, 497, L17
Schlegel, D. J., Finkbeiner, D. P., & Davis, M. 1998, ApJ, 500, 525
Waxman, E., & Draine, B. T. 2000, ApJ, 537, 796
Woosley, S. E. 1993, ApJ, 405, 273